Doppler Reflectometer System for Measuring Rotation Velocity of Fluctuation in GAMMA 10*)

Junko KOHAGURA, Tokihiko TOKUZAWA[1)], Masayuki YOSHIKAWA, Kohei NARITA, Mizuki SAKAMOTO and Yousuke NAKASHIMA

Plasma Research Center, University of Tsukuba, Ibaraki 305-8577, Japan
[1)]*National Institute for Fusion Science, Toki 509-5292, Japan*

(Received 30 November 2015 / Accepted 2 February 2016)

Doppler reflectometry is currently used as a powerful technique to measure the perpendicular (to the magnetic field) velocity of density fluctuation, the radial electric field, and the perpendicular wave number spectrum in many fusion plasma devices. In GAMMA 10 a Doppler reflectometer has recently been installed to measure perpendicular rotation velocity of density fluctuation in the cylindrical plasma. The Doppler reflectometer has an antenna system with a launching/receiving scalar feed antenna and focusing mirrors. By rotating one of the mirrors the tilt angle of the incident microwave can be controlled against the normal of cutoff layers. A frequency synthesizer is used in the range 11.5 - 18 GHz as the stable microwave source of X-mode probing beam for GAMMA 10 plasma having typical peak density $\sim 2 \times 10^{18}\,\mathrm{m}^{-3}$. The first preliminary results of Doppler shifted spectra and radial profiles of the perpendicular velocity of density fluctuations are presented for ICRF start-up plasma with additional ECH. The rotation of fluctuations during additional ECH period is found to become opposite direction comparing to the case of ICRF heating alone.

Keywords: Doppler reflectometer, rotation velocity, fluctuation, microwave, GAMMA 10

DOI: 10.1585/pfr.11.2402022

1. Introduction

Doppler reflectometry is currently used as a powerful technique to measure the perpendicular velocity of density fluctuations, the radial electric field, and the perpendicular wave number spectrum in many fusion plasma devices [1–7]. In Doppler reflectometry the probing microwave beam is tilted with respect to the normal to the cutoff layer. In a slab model with monostatic antenna configuration detecting the diffraction of order -1, the returning signal from the cutoff layer with density fluctuations is Doppler frequency shifted by $f_\mathrm{D} = v_\perp k_\perp/2\pi = 2v_\perp \sin\theta_\mathrm{t}/\lambda_0$. Here, $v_\perp$, $k_\perp$, θ_t and λ_0 are the perpendicular rotation velocity of the fluctuations, the fluctuation wavenumber, the tilt angle and the probing microwave wavelength in vacuum, respectively. In this study we determine f_D by this simple formula. For real geometry ray tracing is often used to obtain the local incident wave vector for calculation of $k_\perp$. The measured fluctuation velocity is determined by the sum of the plasma background $E \times B$-velocity $v_{E\times B}$ and the intrinsic phase velocity of the fluctuation v_ph as $v_\perp = v_{E\times B} + v_\mathrm{ph}$. Generally in tokamaks and helical/stellarators the relation $v_{E\times B} \gg v_\mathrm{ph}$ is realized in the plasma edge, and the ability of Doppler reflectometry to provide radial electric field profile is demonstrated in many works [1, 3, 4, 6].

In the GAMMA 10 tandem mirror device [8, 9] a Doppler reflectometer has recently been installed to measure perpendicular rotation velocity of density fluctuations in a cylindrical plasma at the central cell. In this paper, in Sec. 3, we present details of a newly installed Doppler reflectometer system on GAMMA 10. In Sec. 4 in the experimental results, first, back-scattered microwave spectra are directly captured by a spectrum analyzer to confirm frequency shifts and rotation directions of fluctuations. Second, scanning of tilt angle is performed and effects of an offset of plasma center from its geometrical center on frequency shift measurement are discussed. Finally, radial profiles of perpendicular rotation velocity of fluctuation are presented for a standard, the ion cyclotron range of frequency wave (ICRF) produced plasma together with additional heating phase by electron cyclotron heating (ECH).

2. Experimental Apparatus

GAMMA 10 [8, 9] is a tandem mirror device consisting of an axisymmetric central cell for confining main plasma, minimum-B field anchor cells for stabilizing MHD instabilities, and axisymmetric end mirrors. In the central cell, cylindrical plasma with a length of 5.6 m is formed by solenoid with a uniform magnetic field strength 0.4 T at the midplane. A segmented limiter of 0.36 m in diameter is placed near the midplane of the central cell. The Doppler reflectomter system is installed in the central cell at Z = 0.6 m, where Z is the axial distance from the central cell

author's e-mail: kohagura@prc.tsukuba.ac.jp

*) This article is based on the presentation at the 25th International Toki Conference (ITC25).

midplane.

ICRF are applied to produce and heat plasma. ECH is used for additional heating. Typical plasma parameters in the central cell are as follows. Peak electron density is ~ 2 × 10^{18} m^{-3}, electron temperature and ion temperature are ~ 50 eV and ~ 5 keV, respectively.

3. Doppler Reflectometer System

Figure 1 shows the schematic of Doppler reflectometer system installed on GAMMA 10. The system consists of simple direct conversion microwave circuit using an I-Q mixer and a monostatic antenna.

A scalar horn antenna is used to obtain a symmetrical beam in E- and H-planes. The antenna together with focusing mirrors provides Gaussian beam propagation with the beam radius ω of ~ 85 mm at the plasma edge. Here ω is the beam radius at which the electric field falls to 1/e of its maximum value. By rotating one of the mirrors with a launching angle θ_l (its positive direction is indicated by the arrow in Fig. 1), the tilt angle θ_t of the incident microwave can be controlled against the normal of cutoff-layer surfaces.

A frequency synthesizer (FSW-0020, Phase Matrix, Inc.) is used as the stable microwave source of X-mode probing beam in the range of 11.5 - 18 GHz for GAMMA 10 plasma having typical peak density ~ 2×10^{18} m^{-3}. The I-Q mixer combines the reference signal from the synthesizer and the back-scattered signal from plasma and produces in-phase ($I = A\cos\phi$) and quadrature ($Q = A\sin\phi$) signals. The signals are sampled at 1 MHz by a fast digitizing oscilloscope. A spectrum analyzer (FSW-26, Rohde & Schwarz) is also used for direct observation of a frequency spectrum of back-scattered signal.

In the present study in Secs. 4.2 and 4.3, f_D was determined by a simple weighted spectrum mean technique using the I-Q mixer signals [10]. That is, a sliding fast Fourier transform (FFT) with Hanning window is applied to the complex signal I + iQ to obtain a double-sided power spectrum $S(f)$. Then a weighted spectral mean defined

$$f_d = \frac{\sum f \cdot S(f)}{\sum S(f)},$$

is obtained as the Doppler frequency. A set of f_d during 20 ms steady state period for ICRF phase (10 ms for ICRF+ECH phase) is averaged to obtain the final value of Doppler frequency. The standard deviation from this average was taken as the error.

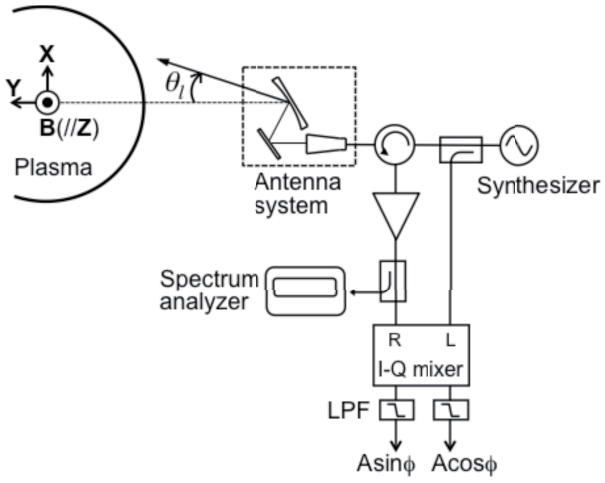

Fig. 1 Schematic of Doppler reflectometer system installed at the GAMMA 10 central cell.

4. Experimental Results

4.1 Rotation direction of fluctuations

Doppler shifted power spectra are directly observed by the spectrum analyzer to confirm frequency shifts and rotation directions of fluctuations with different heating conditions. Figures 2 (a) and 2 (b) show the captured spectra with a probing frequency of 13.7 GHz and the launching angle θ_l of +2° and −3°, respectively. Although all the spectra in Fig. 2 show the influence of the zeroth order of reflection, they clearly have asymmetric structures with respect to the probing microwave frequency. Doppler frequencies calculated by the weighted mean method are indicated by the vertical lines. In Fig. 2 (a), for a typical ICRF plasma the spectrum (the thin line) shows red-shifted feature for θ_l = +2°, indicating an azimuthal propagation of detected fluctuations in the electron diamagnetic direction (see the direction of B in Fig. 1). When an additional

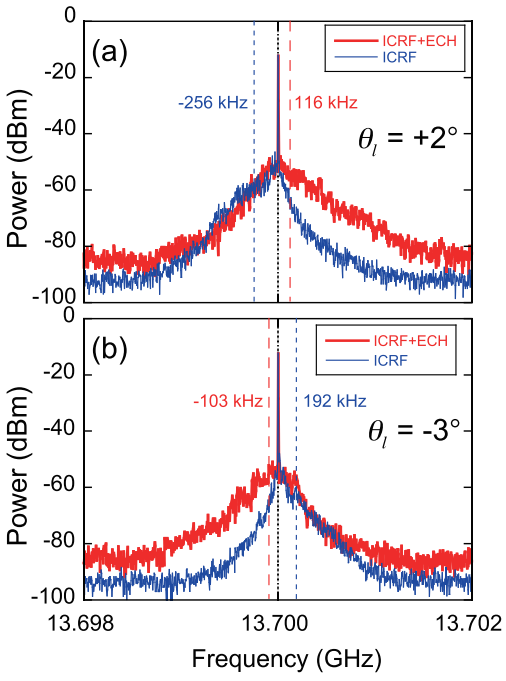

Fig. 2 Directly observed back-scattered microwave spectra of the launching angle (a) +2° and (b) −3°. Thin lines are for ICRF plasma, while thick lines are for additional heating phase by ECH.

ECH is applied to the ICRF plasma, the feature of spectrum turns from red shift to blue shift (the solid line); this suggests the propagation direction is changed to the ion diamagnetic drift direction.

In Fig. 2 (b) as the Doppler shift of the ICRF plasma is positive (blue shift) for the negative θ_l, this again confirms the propagation of the fluctuations in the electron diamagnetic direction. In the ECH period the spectrum shift to lower frequency suggests the change in the propagation direction.

4.2 Tilt angle scan

In another series of ICRF plasma discharge, frequency shift f_D of a series of spectra scanning the tilt angle θ_t is obtained with fixed probing frequency as shown in Fig. 3 (a). Here, θ_l of 0°, ±1°, and ±2° correspond to θ_t of 0°, ±5.6°, and ±11.2° for 11.9 GHz, and 0°, ±6.6°, and ±13.2° for 13.7 GHz, respectively. In Fig. 3 (a), the frequency shift changes almost linearly with θ_t. As the frequency shift can be described by $f_D = v_\perp k_\perp/2\pi = 2v_\perp \sin\theta_t/\lambda_0$, the linear property in Fig. 3 (a) in the range $\sin\theta_t \approx \theta_t$ suggests a constant $v_\perp$ for different $k_\perp$ selected by changing θ_t.

In an ideal condition f_D as a function of θ_t is expected to trace a straight line passing through the origin, however, the frequency shifts in Fig. 3 (a) have finite values at $\theta_t = 0$. This can be due to several reasons, for example, an antenna misalignment, a launching angle setting error, and a shift of plasma position from its geometrical position.

It would be of interest to consider the effect of an offset of plasma center on frequency shift measurement. If the center of a cylindrical plasma has Δx and Δy offset with respect to its geometrical center along X and Y axes, respectively, the resulting actual tilt angle is deviated from the setting tilt angle [see Fig. 3 (c) for the geometric configuration and Fig. 1 for the definition of the axes]. Numerical examples of this effect in our geometrical configuration for the probing frequency of 11.9 GHz at the plasma radius r ~18 cm are displayed in Fig. 3 (b) where the sine of the actual tilt angle θ_{inc} is plotted versus the setting tilt angle θ_t with several offset values shown in mm unit. Note that here we consider the tilt angle in vacuum without refraction. Non-offset case (*i.e.*, $\theta_t = \theta_{inc}$) is shown by the open circles. In other cases Δy is set to −10 mm. When the plasma center is shifted downward ($\Delta x < 0$) θ_{inc} becomes smaller than θ_t. Assuming that $v_\perp$ is constant for different $k_\perp$ on a same cutoff layer, the corresponding measured frequency shift with $\theta_{inc} < \theta_t$ is smaller than that in the non-offset configuration. On the other hand, if the plasma center is shifted upward ($\Delta x > 0$) θ_{inc} becomes larger than θ_t. It is noted that the effect of Δy on the frequency shift is negligible comparing to that of Δx. To explain the minus offsets of f_D measured at $\theta_t = 0$ in Fig. 3 (a) the plasma center is supposed to be at a lower side of the geometrical center, however, in this experiment soft x-ray tomography data shows that the center of x-ray distribution is shifted by $\Delta x \sim +25$ mm and $\Delta y \sim -10$ mm. Therefore to explain

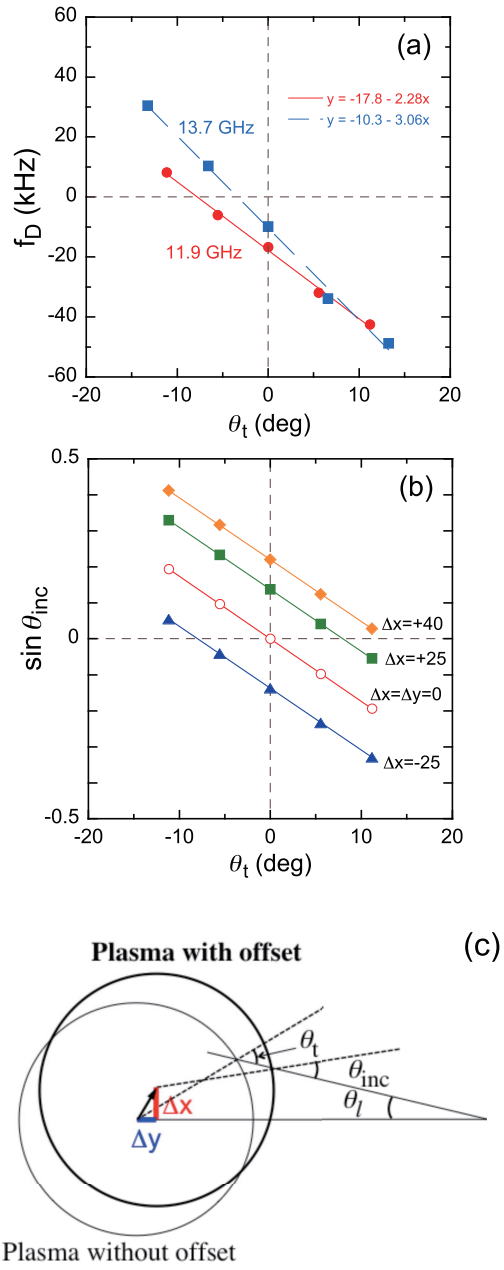

Fig. 3 (a) Frequency shift as a function of the tilt angle with probing frequency of 11.9 and 13.7 GHz. (b) Sine of the actual tilt angle θ_{inc} versus the setting tilt angle with several offset values of plasma center position. (c) Geometric configuration for calculation in Fig. 3 (b).

the result of the present experiment other effects should be considered. Nevertheless, in another viewpoint it is worth noting that Doppler reflectometry is capable of observing such an offset of plasma position by scanning tilt angle.

4.3 Perpendicular velocity profile

Probing frequency scans have been performed to measure radial profile of frequency shift and to obtain perpendicular velocity profile of fluctuations.

Figure 4 shows radial profiles of the perpendicular velocity measured at $\theta_l = +2°$ in only ICRF phase (squares)

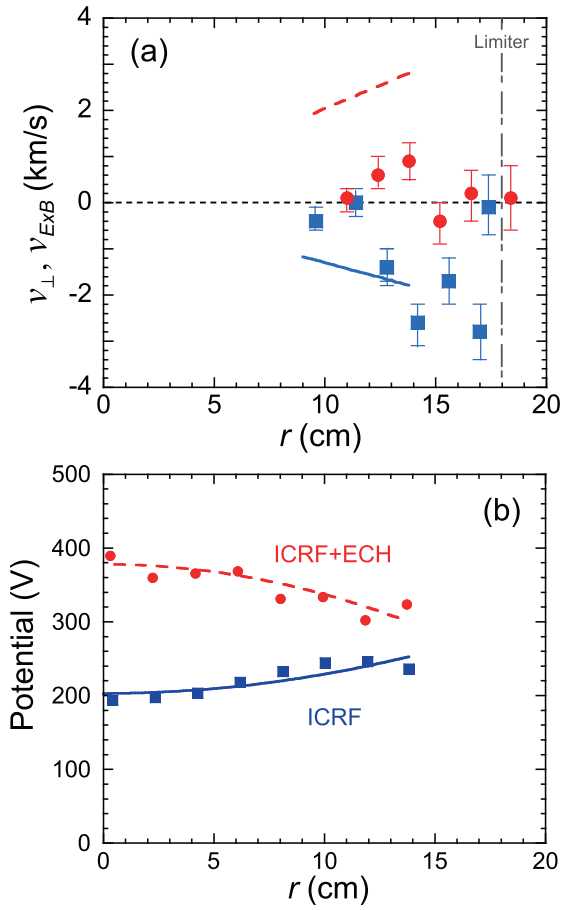

Fig. 4 (a) Radial profiles of the perpendicular velocity of fluctuation are shown in ICRF phase (squares) and ICRF+ECH phase (circles), respectively. Solid and dashed lines are $E_r \times B$ velocity obtained using the potential profile shown in Fig. 4 (b) in ICRF phase and ICRF+ECH phase, respectively.

and with additional heating phase with ECH (circles). The measured radial position is determined from the cold plasma approximation for the cutoff using density profiles measured by a microwave interferometer. In ICRF plasma, the frequency shifts indicate that fluctuations propagate in the electron diamagnetic direction (as described in Sec. 4.1) and have large velocity of 1 - 3 km/s near the plasma edge at plasma radius r = 12 - 17 cm, and small velocity at $r < \sim$11 cm. On the other hand, when the ECH is applied the rotation velocity of fluctuations changes its direction to the ion diamagnetic direction at $r <$ 15 cm and the velocity is $< \sim$ 1 km/s. At $r >$ 15 cm the velocity is almost zero or small comparing to that in the ICRF period. At $r \sim$18 cm where the limiter is installed, the rotation velocity becomes very small in either case.

Figure 4 (b) shows the potential profile of the central cell measured by a heavy ion beam probe (HIBP) [9] in the ICRF phase (squares) and in the ICRF+ECH phase (circles). Parabolic potential profile shown as the curves is assumed to fit the data in Fig. 4 (b) to estimate the radial electric field E_r, then $E_r \times B$ velocity is calculated.

In Fig. 4 (a) the obtained $v_{E\times B}$ in the ICRF phase and in the ICRF+ECH phase are presented as the dashed and the solid lines, respectively. In the ICRF period, at around r = 13 - 14 cm the perpendicular velocity of fluctuation is relatively close to the value of $v_{E\times B}$, however, at $r <$ 12 cm $v_\perp$ has small value comparing to $v_{E\times B}$. In the ICRF+ECH period, as the potential profile changes its shape from well type to hill type, the direction of $v_{E\times B}$ is inverted. Although the direction of the velocities $v_\perp$ and $v_{E\times B}$ is the same at r = 12 - 14 cm, $v_\perp$ is smaller than $v_{E\times B}$. The potential profile data in Fig. 4 (b) is rather dispersed especially in the ICRF+ECH period and the estimated E_r may include some amount of error, nevertheless, a discrepancy seems to exist between $v_\perp$ and $v_{E\times B}$ suggesting the fluctuation phase velocity in the electron diamagnetic direction may not be insignificant. As the HIBP can measure potential only $r <$ 14 cm, we need other diagnostics, for example spectroscopy, to discuss the components of $v_\perp$ in the edge region r = 14 - 18 cm. On the other hand, GAMMA 10 has an open magnetic field end regions where the radially and azimuthally segmented end plates [9] are installed. By applying bias voltage to the end plates the shape of the potential profile can be controlled and hence the radial electric field profile can be changed in the central cell. Such kind of experiments will help to test and understand the ability of Doppler reflectometry.

Acknowledgments

The authors would like to acknowledge the members of the GAMMA 10 group, University of Tsukuba, for their collaboration in the experiments. This work is performed with the support and under the auspices of the NIFS Collaboration Research program (NIFS14KUGM086, NIFS14KUGM099). This work is partially supported by JSPS KAKENHI (No. 26630474).

[1] M. Hirsh *et al.*, Plasma Phys. Control. Fusion **43**, 1641 (2001).
[2] G.D. Conway *et al.*, Nucl. Fusion **46**, S799 (2006).
[3] J. Schirmer *et al.*, Nucl. Fusion **46**, S780 (2006).
[4] P. Hennequin *et al.*, Nucl. Fusion **46**, S771 (2006).
[5] T. Tokuzawa *et al.*, Plasma Fusion Res. **9**, 1402149 (2014).
[6] N. Oyama *et al.*, Plasma Fusion Res. **6**, 1402014 (2011).
[7] T. Happel *et al.*, Rev. Sci. Instrum. **80**, 073502 (2009).
[8] Y. Nakashima *et al.*, Fusion Sci. Technol. **68**, 28 (2015).
[9] M. Yoshikawa *et al.*, Nucl. Fusion **53**, 073031 (2013).
[10] G.D. Conway *et al.*, Plasma Phys. Control. Fusion **47**, 1165 (2005).